

Concept Design of a Smart Haptic Suit for a Biological Signal Recognition and Feedback to Human Body Movements

Dongchan Lee

IAE, 175-28, Goan-ro 51 beon-gil, Baegam-myeon, Cheoin-gu, Yongin-si, Gyeonggi-do, Korea

***Corresponding Author:** Dongchan Lee, IAE, 175-28, Goan-ro 51 beon-gil, Baegam-myeon, Cheoin-gu, Yongin-si, Gyeonggi-do, Korea.**Received date:** January 12, 2024; **Accepted date:** January 17, 2024; **Published date:** January 26, 2024**Citation:** Dongchan Lee, (2024), Concept Design of a Smart Haptic Suit for a Biological Signal Recognition and Feedback to Human Body Movements, *Clinical Research and Clinical Trials*, 9(2); DOI:10.31579/2693-4779/179**Copyright:** © 2024, Dongchan Lee. This is an open access article distributed under the Creative Commons Attribution License, which permits unrestricted use, distribution, and reproduction in any medium, provided the original work is properly cited.

Abstract:

The ultimate purpose of monitoring bio-signals in the form of individually tailored clothing is to monitor an unconstrained bio-signals during the wearer's physiological activities and provide freedom of movement, thereby eliminating inconvenience in workspace of HMI (Human-Machine Interaction) or HRI (Human-Robot Interaction), and healthcare life. In the form of smart clothing for human collaboration industries or everyday life, there is a need to provide new sensitive and high accurate functions to the wearer while also faithfully performing the functions of existing clothing. In this respect, auxetic pattern-based sensors and actuators can be said to be one of the most promising candidates to be combined with smart wearable technology. There is an emerging need to research the concepts of these new sensors and actuators and present a paradigm for clothing research on innovative smart haptic suits. Accordingly, there is a need for a concept of smart haptic system suitable to meet the conditions of sensors and actuators with improved sensitivity, conductivity, and receptivity that can have characteristics such as microporosity, flexibility, and large surface area of nano and micro web structures. When measuring a bio-signal sensing and motion feedback using an electro-active structural pattern, the signal waveform can be confirmed to have a similar signal waveform to the measured signal through direct visual evaluation, and muscle signals for each body part can be measured using a commercialized sensor. The same signal can be confirmed. Through Pearson's correlation analysis using statistical analysis techniques, signal data between nano and micro web structure-based respiration sensors and existing respiration sensors showed significant correlation with each other, indicating respiration obtained from nano and micro web-based sensors. A theoretical model which predicts the actuation stroke of the system based on the material properties of the auxetic SMM (Shape Memory Material) and bias components as well as the geometry of the metamaterial system was developed.

Keywords: smart clothing; ergonomic signal monitoring; motion artifact; auxetic pattern electrode; re-modularization

1. Introduction

Bio-monitoring smart clothing for human-robot interaction, human-machine interaction and health care is a new type of smart haptic clothing that combines the human body, with BT and IT functions. By attaching various devices that can check biological signals, signals such as the wearer's breathing or heart rate or body movements can be detected, allowing the wearer's bio-signals to be checked in a personalized way in daily life. Bio-monitoring smart clothing is a type of smart clothing that is essential for future daily life, where interest in human interaction industries or health is expected to increase. Bio-monitoring systems are evolving from measuring bio-signals using bio-medical devices such as thermometers or pulse monitors to measuring bio-signals through sensors integrated into clothing or bands. This phenomenon is changing from existing bio-medical devices to smart haptic suits that can be worn in daily life as interest in health increases and the desire to check one's health status at any time increases. The wearable system consists of four key elements. These include a 'sensing system' that detects physical and chemical changes in the human body, a

'monitoring system' that provides measured biometric information, an 'analysis system' that presents new health indicators based on the analysis of transmitted data, and a health status message to the wearer. It is a feedback system that notifies changes, etc. Wearable technology [1]. soft robotics [2]. human-robot interaction [3,4] and human-machine interaction [5]. have sparked a growing interest in embedded soft devices. Accordingly, various methods have been proposed to manufacture soft sensors that can be integrated into smart clothing systems [6,7]. In the future, for bio-monitoring smart clothing to become popular in everyday life, it is important that the core elements of the wearable system develop evenly to provide the maximum performance required by consumers, but the selective combination of the core elements for this is also very important [8-12].

The most important thing is to make the sensing system wearable, that is, to make the sensor wearable. Most have three functions for acquiring bio-signals. One is to measure the respiratory rate using an EMG sensor, the other

is to measure the electrocardiogram using a medical ECG sensor, and the third is a system to measure the degree of movement through a motion measurement sensor such as an IMU. It consists of a memory card that stores data and a system that transmits, analyzes, and provides feedback. However, it is a block-based model made from a combination of structure and electronic devices, rather than being completely integrated. Information such as speed and exercise distance input through the heart rate and IMU sensor is displayed on the computer in real time, allowing you to know what level of intensity you are exercising. In addition, to check whether the electrical resistance changes depending on the degree of elongation of the structure, the change in electrical resistance can be measured with a multimeter, and then the change in electrical resistance of the structure according to the elbow angle can be measured in real time while wearing an arm sleeve. The electrical resistance values appear different even at the same angle when the structure is stretched (arm flexion operation) and contracted (arm extension operation). The reason is that when the arm is bent, the sensor attached to the elbow is stretched and receives a forced force in the opposite direction to its original shape, so the change in resistance occurs slowly, and when the arm is extended again, the structural sensor returns to its original shape. Changes in electrical resistance can be used at high speeds. If the principle of this motion measurement sensor is applied to other body parts besides the arms, it can be used to predict the body motion size of that part through clothing. When monitoring ECG and EMG signals, electrodes woven or woven from conductive metal thread are used as bioelectrodes. The method of sensing the microcurrent coming from the heart and transmitting it to the output device is the same as the electrode commonly used in medical institutions, but it is meaningful in that it is human-friendly and can be worn at all times [13-19].

In this paper, we analyzed key element technologies for the development of smart haptic suits by dividing them into key elements in the development of bio-monitoring smart clothing and e-textiles, the type of sensing system, electrocardiogram measurement, respiration measurement, and motion measurement. As mentioned in the introduction, bio-monitoring systems are evolving from non-wearable systems such as thermometers or pulse meters to wearable systems such as clothing or bands. This is an inevitable choice to meet human needs for high acceptability, high sensitivity, and convenience of wearing in the concept of a smart haptic suit that can analyze behavior and check bio-signals in daily life and provide muscle support anytime and anywhere. We intend to compare and examine the feasibility and feasibility of use as a smart textile by manufacturing conductive nano and micro webs as textile sensors using nanotechnology and metal coating techniques. Nano and micro web structures have characteristics such as porosity, flexibility, and large surface area, which can greatly contribute to improving conductivity. This is suitable to meet the conditions of the sensor, so based on this, it is expected to be suitable as a textile sensor. It is expected. Through this, we measure biological signals such as EMG, ECG and respiratory rate, verify the quality of the signal by comparing and analyzing it with signals obtained through existing non-textile sensors, and provide an integrated soft actuator function based on this.

2. Auxetic Tactile Sensor for Smart Haptic Suit

2.1 Design Concept of Soft Sensor for Smart Haptic Suit

If the optimal conditions for producing conductive nano- and micro-web textiles with conductive polymers using sensors are discovered, it will be possible to develop textiles that minimize clothing wearers' resistance and naturally perform their unique functions within a smart clothing system. Flexible and soft sensors are currently the most studied component of smart clothing, but most studies simply focus on flexibility, and research on constructing smart clothing systems using nanomaterials is minimal.

Accordingly, it can be said that research is needed to develop nano and micro web textiles that are flexible, lightweight, and highly conductive as sensors. The ultimate purpose of monitoring biological signals in the form of clothing is to monitor the wearer's physiological activity time. This provides new functions to the wearer in the form of smart clothing for HMI, HRI and everyday life while faithfully performing the functions of existing clothing. There is a need to do it. In this respect, nano or micro materials can be said to be one of the most promising candidates to be combined with wearable technology. So far, metal materials have been mainly used in research on the use of conductive materials as clothing materials, but there is an emerging need to research new materials and present an innovative paradigm for clothing research

The bio-signal measurement module receives bio-signals through three electrodes, and includes a hardware filter to block various noises, an amplifier circuit to amplify the bio-signals, and DSP (Digital Signal Processing) to filter software noise signals and convert the signals into data. It consists of a processor and a Bluetooth module for wireless data transmission. Accordingly, by using nano or micro technology and metal coating techniques, conductive nano and micro webs were manufactured as textile sensors and used as smart textiles. Nano and micro web structures have characteristics such as microporosity, flexibility, and large surface area, which can contribute to improving conductivity. Since this is suitable to meet the sensor conditions, it is expected to be suitable as a textile sensor based on this, and the following research contents can be included in the development of a smart haptic suit: (a) Fabrication of conductive nano and micro web samples based on metallic nanomaterials and textile sensorization: Fabrication of conductive nano and micro web structures/Excellent electrical properties and improved tensile strength/Improved signal transmission ability of nano and micro web-based sensors/Nano and micro web structures Checking the washing and abrasion resistance of web-based sensors. (b) Fabrication of conductive polymer-based conductive nano- and micro-web samples and textile sensorization: Fabrication of composite-based conductive nano- and micro-web structures using various conductive materials / Fabrication of conductive polymer-based conductive nano- and micro-web structures using various conductive materials. (c) Clothing evaluation and textile-based bio-signal monitoring system: Wearing evaluation is conducted on dummies and subjects, and the suitability is verified using statistical techniques by comparing signals with existing bio-signal measurement devices/nano and micro web-based biometrics. Development of signal monitoring smart clothing/To develop nano- and micro-web-based electrocardiogram electrodes Resistance characteristics such as line resistance and sheet resistance for bio-signal recognition/High-soluble gauge ratio to develop nano- and micro-web-based respiration sensors

2.2 Design of Auxetic Tactile sensor

Auxetics are defined as materials or structures with the elastic property of negative Poisson's ratio (NPR): when the material is stretched in one direction, it expands in one or more transverse directions as well [20,21]. This differs from most materials/structures that typically show a contraction in the perpendicular direction to the stretched direction. Wearable electronic devices can monitor various strains, which is beneficial to human healthcare, medical rehabilitation, soft robotics, human-robot interactions, and human-machine interactions. Strain sensors have received more attention owing to their good conformality, integrability and wearability. To guarantee widespread application, wire strain sensors should possess high sensitivity, high stretchability, and excellent durability. The sensitivity, indicated by the gauge factor (GF), is evaluated by the following equation.

$$GF = \frac{\Delta R/R_0}{\Delta L/L_0} = \frac{\Delta R}{R_0 \varepsilon} = \frac{\Delta C}{C_0 \varepsilon} \approx 1 + 2\nu \quad (1)$$

where $\Delta R / R_0$, $\Delta C / C_0$, R , C , ε and ν denote the relative resistance change, the relative capacitance change, real-time resistance, real-time capacitance, tensile strain, and Poisson's ratio, respectively. When an increasing force (ΔF) applied onto one of the sensing units, the capacitance or resistance is measured for each increment. The sensitivity S of a capacitance or resistance or magnetic flux can be expressed as,

$$S = \frac{\Delta C/C_0}{\Delta F} = \frac{1}{d_0} \frac{\Delta d}{\Delta F} = \frac{\Delta B}{\Delta F} \quad (2)$$

Where ΔB is the amount of the change in the sensed-magnetic field before and after strain applied, and ΔF is the applied force change? Among the above-mentioned indicators, stretchability and durability are especially important because they ensure large stress loading and stable output of sensing signals after repeated deformation. Although resistance change increases sharply under a large strain, irreversible structural damage appears, and repeated cycling induces a viscoelastic effect, which results in potential fracture and poor durability. To achieve controllable high sensitivity as well as good stretchability and durability, a novel design concept of auxetic materials/structures is integrated with a magnetic field sensing system in this work. The sensitivity of our strain sensors was tuned by tailoring the geometric dimensions of the auxetic structure. Upon mechanical loading, the sensors showed a structural deformation effect (i.e., longitudinal stretching accompanied by transverse structural deformation), which resulted in good stretchability and durability. As the strain increased, continuous stretching produced high sensitivity. The typical auxetic structures are listed in Table 1 [22]. Three architectures were explored as the fundamental pattern. The structural Poisson's ratio(ν) is calculated using eq. (3):

$$\nu = -\frac{\varepsilon_y}{\varepsilon_x} \quad (3)$$

where ε_x and ε_y represent the x-direction strain and y-direction strain.

As shown in Figure 1-(b), Eco-flex (1:1 mixture of casting and hardening materials) and PDMS (10:1 mixture of casting and hardening materials) were mixed at a 1:1 ratio for four auxetic sensors shown in Figure 1-(a). To prevent curing rejection, it was important to thoroughly mix each solution separately before combining them. Afterwards, NdFeB particles were added in a 1:1 weight ratio to the mixed silicone solution. In a vacuum chamber, bubbles were removed from the resulting mixture, which was injected into a mold created through 3D printing. To avoid the formation of a pseudo membrane that could reduce the efficacy of the sensor, the solution was carefully injected using a syringe instead of simply pouring and molding it. Next, the mold containing the solution was placed in an oven at 55 degrees Celsius for 3 hours. Once cured, the material was removed from the mold using tweezers. At a 10% tensile strain, the sum of factors for the re-entrant hexagon was 77uT, for the modified re-entrant hexagon it was 90uT, for the rotating triangular plates it was 99uT, and for the rotating square plates it reached 169uT, as shown in Figure 1-(C). Furthermore, to assess the Poisson's ratio of each sample, the width and length of the samples were measured both before and after the tensile test. The calculated Poisson's ratios were -0.1, -0.12, -0.66, and -0.75, respectively. An auxetic structure requires less force to obtain the same sensing value as a regular rectangular sensor of the same size. Additionally, when stretching the sensor over the same length, an auxetic structure demands less force. In Figure 2-(A), it can be observed that normal samples required approximately force of 1.0 N to induce a displacement of 100uT, whereas the auxetic samples required only about 0.2 N of force to achieve the same displacement. Furthermore, as shown in Figure 2-(B), when subjected to the same amount of tensile force, it was evident that the auxetic samples required less force compared to the normal samples. This is advantageous for applying sensors to small joints such as finger joints. We prepared a 33mm auxetic sensor and a regular rectangular sensor, both fixed at the length of 5mm of each sensor, in the same configuration. The calculated sensitivity using equation (2) shows (110 μ T)/(0.2 N) = 550 for the auxetic sensor, and (25 μ T)/(0.2 N) = 125 for the conventional sensor [22].

Auxetic Structure	Shape	Poisson's ratios	Young's modulus
Re-entrant hexagon [20,21] $h = 2l, n = 8$		$\nu_{12} = -\frac{l \sin^2 \theta}{(h + l \cos \theta) \cos \theta}$ $\nu_{21} = -\frac{(h + l \cos \theta) \cos \theta}{l \sin^2 \theta}$	$E_1 = n E_s \left(\frac{t}{l}\right)^3 \frac{\sin \theta}{(h/l + \cos \theta) \cos^2 \theta}$ $E_2 = n E_s \left(\frac{t}{l}\right)^3 \frac{(h/l + \cos \theta)}{\sin^3 \theta}$
Modified Re-entrant hexagons (with diamond-shaped cells) $h = 2l, n = 4$		$\nu_{12} = -\frac{l \sin^2 \theta}{(h + l \cos \theta) \cos \theta}$ $\nu_{21} = -\frac{(h + l \cos \theta) \cos \theta}{l \sin^2 \theta}$	$E_1 = n E_s \left(\frac{t}{l}\right)^3 \frac{\sin \theta}{(h/l + \cos \theta) \cos^2 \theta}$ $E_2 = n E_s \left(\frac{t}{l}\right)^3 \frac{(h/l + \cos \theta)}{\sin^3 \theta}$

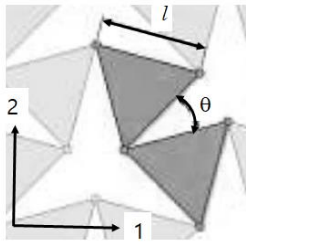
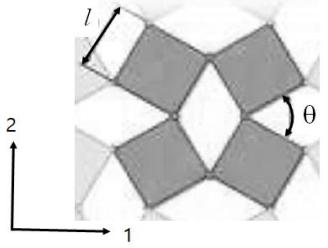
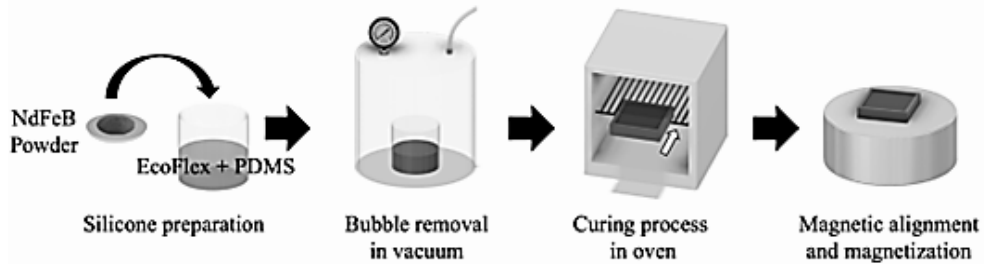
<p>Rotating Triangular Plates (Equilateral) [23]</p>		$v_{12} = v_{21} = -1$	$E_{1,2} = k_h \frac{4\sqrt{3}}{l^2 [1 + \cos(\frac{\pi}{3} + \theta)]}$
<p>Rotating Square Plate [24]</p>		$v_{12} = v_{21} = -1$	$E_{1,2} = k_h \frac{8}{l^2 [1 - \sin(\theta)]}$

Table 1: Characteristics of typical auxetic structure

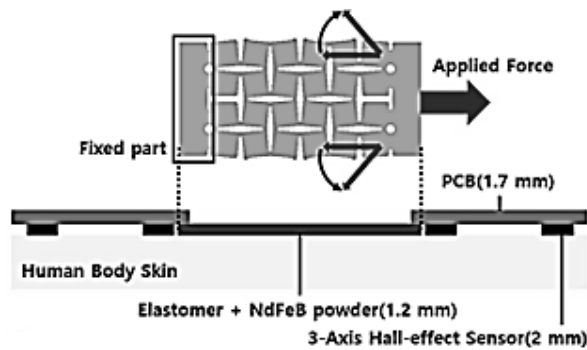
※ Properties of unit cell material: E_s : Young's modulus, ν : Poisson's ratio, k_h : stiffness constant, n : no. of cell strut of re-entrant hexagon, $B=2l\sin\theta$, $H=h+2l\cos\theta$

Material	Density (kg/m ³)	Young's Modulus (MPa)	Poisson's Ratio
TPUs	1200	15.31	0.48

Table 2: Material properties



(a)



(b)

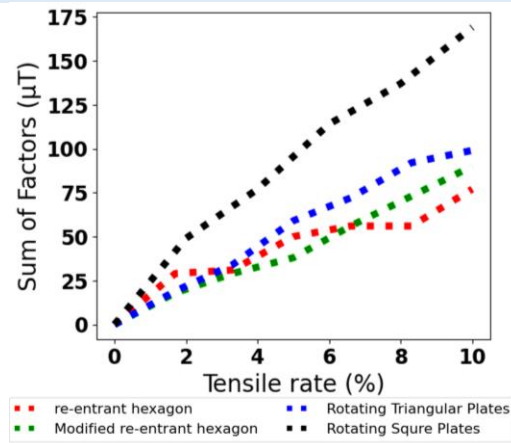


Figure 1: Experimental schematics: (A) Fabrication process of auxetic sensors, (B) Illustration of auxetic sensors, (C) Sum of factors for tensile ratio and Poisson's ratio is -0.1, -0.12, -0.66, -0.75 for the sensors of auxetic patterns (re-entrant hexagon, modified re-entrant hexagon, Rotating Triangular Plates and Rotating Square Plate)

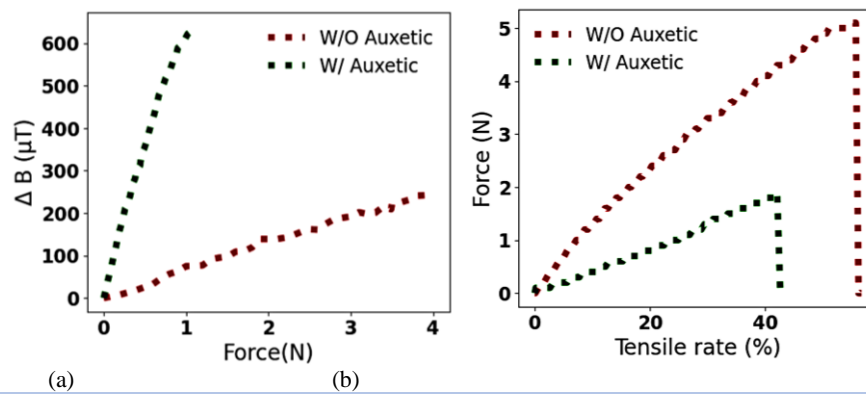


Figure 2: Operation of sensors with an auxetic matrix and without an auxetic matrix under different external tensile forces (a) Magnetic Field Variation with Force, (b) Tensile rate Due to Force.

3. Auxetic Tactile Actuator for Smart Haptic Suit

3.1 Design Concept of Auxetic SMM

The importance of wearable devices continues to increase due to their ability to provide real-time body feedback, offer a variety of functions, and provide a comfortable experience for the wearer. To improve wearability, an auxetic SMM actuator can be developed by manufacturing a shape memory material such as shape memory alloy (SMA) or shape memory polymer (SMP) with an auxetic structure that is lightweight and changes its physical shape and stiffness depending on temperature. This wearable actuator has the characteristic of increasing wearability and convenience for the wearer's 3D curved human body, and by applying the auxetic SMM wearable actuator as a wearable haptic, virtual senses are provided through thermal and mechanical feedback. can be experienced, and through this, the auxetic SMM actuator can be used as a wearable haptic. The transition from the martensite (low temperature) phase to the austenite (high temperature) phase in auxetic

SMM does not occur instantaneously in a specific temperature range but proceeds gradually over a temperature range. Figure 3 shows the relationship between displacement and temperature, where the austenite start temperature is shown as A_s , the austenite end temperature is shown as A_f and the martensite start and end temperatures are shown as M_s and M_f , respectively. In the temperature range indicated by ΔT , the alloy consists of a mixture of austenite and martensite. As can be seen from this, there is virtually no change in length below A_s , and as SMM is heated, no further change in length occurs above A_f . Similarly, substantially no change in length occurs above M_s immediately after cooling, and no further change in length occurs below M_f . Typically, there is significant hysteresis in the length-temperature curve (Figure 3, 4). The resistance within the shaded region between R_{min} and R_{max} can be used as an analog for the auxetic SMM temperature, and the resistance-temperature curve exhibits significant hysteresis. Therefore, the transformation rate between the two phases can be inferred based only on the resistance value without directly measuring the temperature.

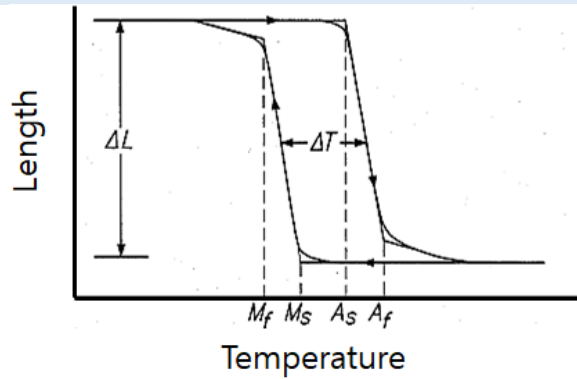


Figure 3: Relationship between auxetic SMM stroke and temperature

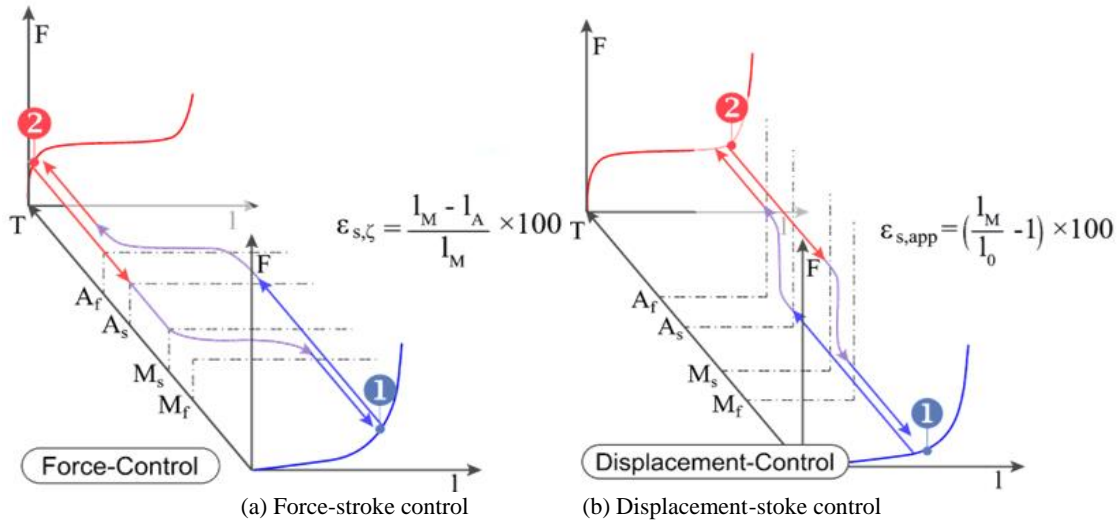


Figure 4: Relationship of force & displacement with auxetic SMM stroke: ① non-deformation state, ② force and deformation state

Auxetic shape memory material actuators can be described as a control and sensing mechanism, generating control information for the actuator using a control scheme that utilizes resistive feedback and changes in actuator resistance over time as the electrical signals are applied to the actuator. These control and sensing mechanisms perform position control functions, measure the load on the actuator, detect a signal collision or mechanical failure and system errors in the actuator, and provide compensation for the actuator. In a preferred control mechanism, measurement of the discharge time of a capacitor connected in parallel with the actuator is used to measure the resistance of the actuator. The model predicts the operating output based on the balance of forces created by the interaction between the auxetic SMM and the bias component and is based on several assumptions: (a) The auxetic geometry has only a kinematic effect on the deformation of the system and does not contribute to the internal energy in terms of the work done on the actuator. This means that the influence of factors such as friction and the structural hinges and weight of the structure is negligible. (b) The stress-strain behavior of the auxetic SMM component in the martensitic phase can be expressed as a trilinear model with each line representing the twin martensitic state (*M*), the transition state (*T*), and the twin martensitic state (*DM*), respectively (Figure 5). The austenite state can be represented by a linear model. (c) Upon activation/heating, the auxetic SMM component completely converts from martensite to austenite phase. This is usually the case for auxetic SMM systems with small cross-sectional areas, such as wires and strips, which are activated through the thermal effect. (d) The model is static, so the deformations of both the auxetic SMM and the bias components are elastic, fully recoverable, and unaffected by the activation rate. When

activated using an electric current, the transformation from martensite to austenite phase occurs almost instantaneously

3.2 Numerical Descriptions of Auxetic SMM

For a prototype of auxetic SMM actuator, it is necessary to develop a numerical expression that can be used to predict the actuation output of the system as a function of the material properties of the individual components and the overall geometry of system. This actuator consists of three components: a SMM, a bias component, and an auxetic material geometry. Each plays a distinct role in ensuring the overall functioning of the complex system. Auxetic SMM components guide actuation of the system, bias components provide reversibility upon deactivation and reusability of the actuator, and auxetic material geometry controls the actuation stroke and force output of the system in axial and transverse directions. These three components are shown in Figure 5. To maximize the actuation stroke output, the auxetic SMM component is placed at position l_{AB} and the bias component is placed at position l_{CD} . This means that upon activation, the contraction of the auxetic SMM component is counteracted by the stretching of the bias component imposed through the kinematic constraints of the auxetic material deformation mode. Since $l_{AB} > l_{CD}$, this also leads to the total positive operating stroke of the actuator. To quantify the operating stroke of the system, it is necessary to equilibrate the force and displacement of the auxetic SMM and bias components along the l_{AB} direction. Because the auxetic SMM component is aligned along l_{AB} , the force-displacement plots obtained from uniaxial loading of this component can be used directly, as shown in Figure 5. However, this is not the case for the bias component oriented

perpendicular to l_{AB} . Therefore, the force and displacement exerted by the bias component in the direction l_{AB} required to maintain the equilibrium of the system must first be found through the kinematic laws that define the deformation of the auxetic material system. [25-28].

The pre-strain of the auxetic SMM component can be driven by the elastic bias component, which in this case is assumed to be a flexure hinge or compliant systems that deforms linearly over high strains. This means that during actuator assembly, the auxetic SMM component must first be introduced within the system with a predetermined length l_{SMM} , followed by the elastic bias component. For the bias component to pre-stress the SMM component, the initial length l_{bias} in the remainder of the bias component must be less than the length l_{CD} corresponding to the length l_{AB} of the auxetic SMM component. This condition can be expressed as:

$$l_{bias} < \sqrt{4a^2 - l_{SMM}^2} \quad (4)$$

and to integrate the bias component within the actuator, we ensure that the pre-strain applied to the bias component imparts sufficient force to balance the SMM and induce pre-strain in the latter component. The force-displacement relationship of the auxetic SMM component in its martensitic phase is represented by a tri-linear model. The SMM has an initial length of l_{SMA} at rest and the model (shown in figure 3) may be expressed in terms of force (F_{AB}) and total length (l_{AB}) along the line between the points A and B as:

$$F_{AB} = k_M(l_{AB} - l_{SMM}), l_{SMM} \leq l_{AB} < (l_{SMM} + d_T) \quad (5)$$

$$= F_T - k_T(d_T + l_{SMM} - l_{AB}), (l_{SMM} + d_T) \leq l_{AB} < (l_{SMM} + d_{DM}) \quad (6)$$

$$= F_{DM} - k_{DM}(d_{DM} + l_{SMM} - l_{AB}), (l_{SMM} + d_{DM}) \leq l_{AB} \quad (7)$$

where $k_M (= E_M^A/l_{SMM})$, $k_T (= E_T^A/l_{SMM})$ and $k_{DM} (= E_{DM}^A/l_{SMM})$ are the stiffness constants for the twinned martensitic state, transition state and detwinned martensitic state in the uniaxial experiments of SMM wire, respectively, while $F_T (= \sigma_T A)$, $d_T (= \epsilon_T l_{SMM})$, $F_{DM} (= \sigma_{DM} A)$ and $d_{DM} (= \epsilon_{DM} l_{SMM})$ represent the force (F) and displacement (d)

thresholds required to switch from the first to second state (eqs. (5)–(6)) and the second to third state (eqs. (6)–(7)). These three lines represent the force-displacement behavior of the martensitic SMM in the twinned, transition and detwinned state respectively and are valid within the limits defined in the equations.

This numerical modelling of the force-displacement of martensitic auxetic SMM is identical to the analytical method to model uni-axial bias actuator behavior. The equations can be expressed in terms of stiffness constants, transformation displacements and forces rather than Young's modulus, strain and stress for various geometric patterns. In the case of auxetic SMM, these factors may easily be derived directly from basic stress-strain plots in the experimental parts. As shown in Figure 5, the force-displacement behavior of the bias component counteracting the auxetic SMM is represented by a non-linear model along the line AB. This is due to the fact that although the stiffness of the bias component is constant, it is aligned along the line CD, orthogonal to the line AB. The austenitic force-displacement behavior in Figure 5 is represented by the following linear model:

$$F_{AB} = k_A(l_{AB} - l_{SMM}) \quad (8)$$

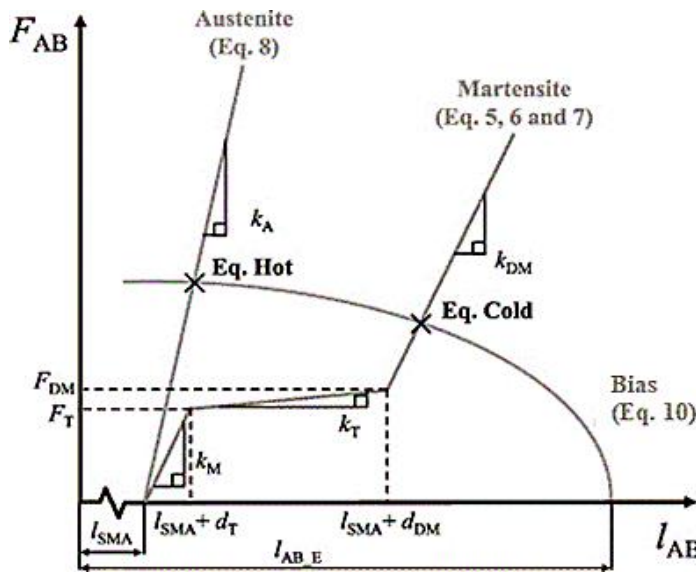
$$F_{CD} = k_{bias}(l_{CD} - l_{bias}) \quad (9)$$

$$F_{AB} = F_{CD} / \tan\theta \quad (10)$$

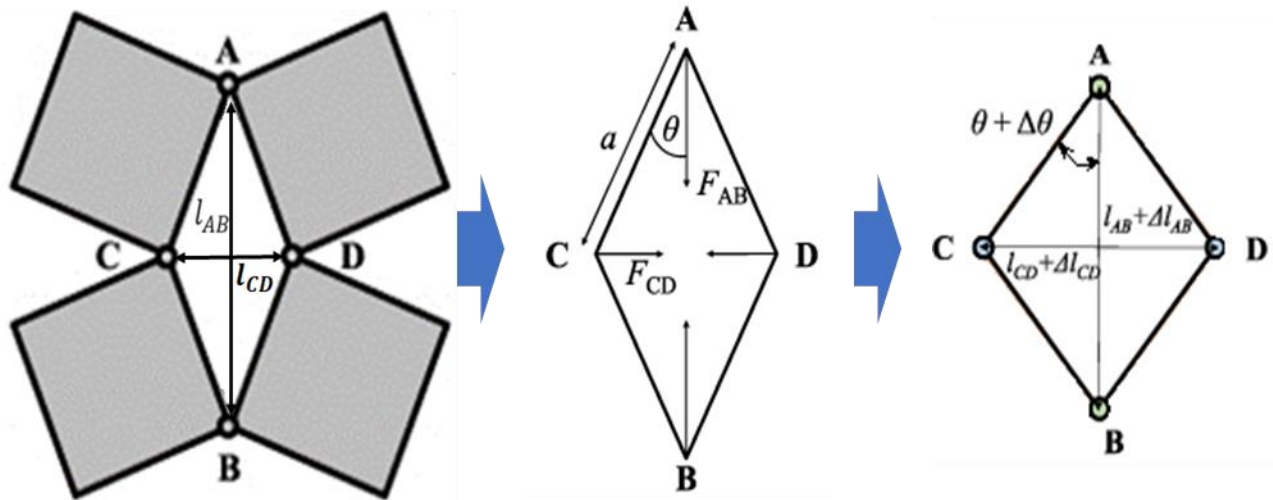
where $k_A (= E_A^A/l_{SMM})$ represents the stiffness constant of the SMA in its austenitic phase. l_{bias} is the initial length of the elastic bias component and k_{bias} is the associated stiffness constant. $\theta = \arccos(l_{AB}/2a)$. $l_{CD} = \sqrt{4a^2 - l_{AB}^2}$.

Eq. (10) is non-linear model for the bias component along the line AB, and $l_{Eq,H} = l_{AB,Eq,H} + l_{CD,Eq,H}$ and $l_{Eq,C} = l_{AB,Eq,C} + l_{CD,Eq,C}$ for the martensitic and austenitic phase of actuator can be used to find the corresponding cold and hot equilibrium global length of actuator. The maximum permissible actuation for a given bias component can be given by,

$$l = l_{AB} + l_{CD} = l_{AB} + \sqrt{4a^2 - l_{AB}^2} \quad (11)$$



(a) Relationship between forces and displacements acting along l_{AB}

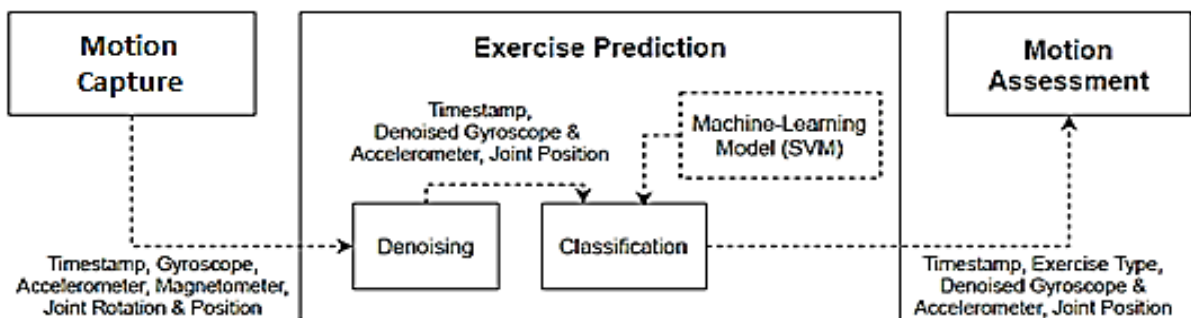


(b) Deformation of unit auxetic cell under tensile loading

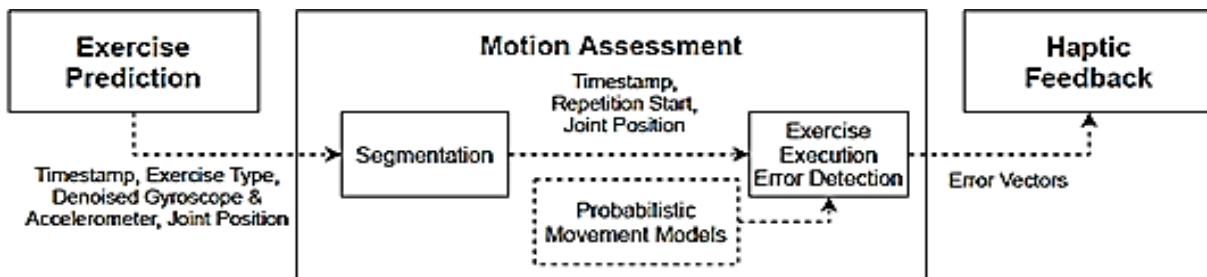
Figure 5: A qualitative plot showing the forces and displacements acting along l_{AB} for the SMM in martensitic and austenitic state and the opposing bias component. The equilibrium points at the SMM hot and cold states are also indicated



Figure 6: Sample schematics of auxetic SMM actuator for arm muscular skeletal motion



(a) Flowchart for exercise prediction



(b) Flowchart for movement assessment

Figure 7: Flowchart for feedback control of smart haptic suit

4 Discussion and Conclusion

In the user-centered smart haptic development technology, there is a need for continued development of integrated technology that can transform electronic devices into clothing. To advance from block-based to embedded and finally to fiber-based technology, new materials such as EAP, nanotechnology, and new technologies such as electrospinning in textile converting technology are the next generation. Active research must be conducted to develop materials. For the elements that make up smart clothing, such as sensors, power supplies, and output devices, to operate efficiently, interconnection technology that considers compatibility, durability, and usability must also be developed. Currently, there are differences in the level of development of clothing-embedded technology for each component of smart clothing. Therefore, standardized standards must be established to achieve effective interconnection between each component. Smart haptic suits are fashion items that must satisfy users in both functional and emotional aspects. Therefore, user-centered technology that reflects the potential needs of consumers requires the integration and interconnection technologies mentioned above. Smart haptic suit using these smart materials can be broadly divided into passive and active types, the latter of which consists of a sensor that can detect environmental changes and an actuator that can respond, and can detect physiological changes in the living body through electrical, magnetic, and A sensor that detects or monitors with optical signals is built or installed in the form of an array chip on a thin polymer sheet, paper, fiber material, or special material sheet. A bio-signal sensitive actuator that operates according to detected bio-signals is built into or installed on the same sheet. In some cases, the detected bio-signal can be communicated with an external digital device to drive an actuator mounted on a separate structure.

Acknowledgement

This research was supported by the Technology Innovation Program (20019115) funded by the Korea Planning & Evaluation Institute of Industrial Technology (KEIT) and the Ministry of Trade, Industry, & Energy (MOTIE, Korea).

References

1. Yin, J, Hinchet, R. Shea. H, and Majidi, C. (2021). Wearable soft technologies for haptic sensing and feedback. *Advanced Functional Materials*, 31(39):2007428.
2. Yasa. O. Toshimitsu, Y. Michelis. M.Y, Jones. L.S, Filippi. M, Buchner. T, et al. (2023). An Overview of Soft Robotics. *Annual Review of Control, Robotics, and Autonomous Systems* 6:1-29.
3. Kyung, K.-U, and Kim, S.-Y. (2019). Soft sensors and actuators for designing new human-robot/machine interaction interfaces, in: 2019 14th ACM/IEEE International Conference on Human-Robot Interaction (HRI): IEEE), 695-695.
4. Pang. G, Yang. G, Heng. W. Ye, Z. Huang, X, Yang. H.-Y, et al. (2020). CoboSkin: Soft robot skin with variable stiffness for safer human-robot collaboration. *IEEE Transactions on Industrial Electronics*, 68(4):3303-3314.
5. Dong, W, Wang. Y, Zhou. Y, Bai. Y, Ju. Z, Guo, J, et al. (2018). Soft human-machine interfaces: design, sensing and stimulation. *International Journal of Intelligent Robotics and Applications*, 2:313-338.
6. Chen. W, Khamis. H, Birznieks. I, Lepora, N.F, and Redmond, S.J. (2018). Tactile sensors for friction estimation and incipient slip detection—toward dexterous robotic manipulation: A review. *IEEE Sensors Journal*, 18(22):9049-9064.
7. Zhao. Z, Hu, Y.-P. Liu, K.-Y, Yu, W, Li, G.-X, Meng, C.-Z, et al. (2023). Recent Development of Self-Powered Tactile Sensors Based on Ionic Hydrogels. *Gels* 9(3):257.
8. Barfield W, Mann S, Baird K, Gemperle F, Kasabach C, Stivoric J, Bauer M, Martin R. and Cho G. (2001). "Fundamentals of Wearable Computers and Augmented Reality"(Ed. by Barfield W. and Caudell T.). Lawrence Erlbaum Press, 471.
9. Carpi F. and Rossi D. D. (2005). Electroactive polymer-based devices for e-textiles in biomedicine. *IEEE Transactions on Information Technology in Biomedicine*, 9(3):295-318.
10. Catrysse M, Puers R, Hertleer C, Langenhove L. V, Egmond H. V. and Matthys D. (2004). Towards the integration of textile sensors in a wireless monitoring suit. *Sensors and Actuators A: Physical*, 114(2-3):302-311.
11. Cottet D, Grzyb J, Kirstein T. and Troster G. (2003) Electrical characterization of textile transmission lines. *IEEE Transactions on Advanced Packaging*, 26(2):182-190.
12. Frank H. W. and Walton T. R. (2003). The lifeshirt. *Behavior Modification*, 27(5):671-691.
13. Gibbs P. T. and Asada H. H. (2005) Wearable conductive fiber sensors for multi-axis human joint angle measurements. *Journal of Neuro Engineering and Rehabilitation*, 2(1):7.
14. Ottenbacher J, Romer S, Kunze C, Grossmann U. and Stork W. (2004). Integration of a bluetooth based ECG system into clothing. *Proceedings of the 8th International Symposium on Wearable Computers*. Washington DC, 186-187.
15. Paradiso R. Loriga G, Taccini N, Gemignani A. and Ghelarducci B. (2005). WEALTHY-a healthcare system: New frontier on e-textile. *Journal of Telecommunications and Information Technology*:105-113.
16. Rossi D. D, Carpi F, Lorussi F, Mazzoldi A, Paradiso R., Scilingo E. P. and Tognetti A. (2003). Electroactive fabrics and wearable biomonitoring devices. *AUTEX Research Journal*, 3(4):180-185.
17. Mark S. and David K. (2005). "Wearable Systems: Global Market Demand Analysis". 2nd Ed., Vol. 2, Venture Development Corporation(VDC), 36-40
18. Wijesiriwardana R, Mitcham K. and Dias T. (2004). Fibre-meshed transducers based real time wearable physiological information monitoring system. *Proceedings of the 8th International Symposium on Wearable Computers*, Washington DC, 40-47.
19. Wijesiriwardana R. (2006). Inductive fiber-meshed strain and displacement transducers for respiratory measuring systems and motion capturing systems, *IEEE Sensors Journal*, 6(3):571-579.
20. Ashby, M.F, and Gibson, L.J. (1997). *Cellular solids: structure and properties*. Press Syndicate of the University of Cambridge, Cambridge, UK, 175-231.
21. Gibson, L.J, Ashby, M.F, Schajer, G, and Robertson, C. (1982). The mechanics of two-dimensional cellular materials. *Proceedings of the Royal Society of London. A. Mathematical and Physical Sciences*, 382(1782):25-42.
22. Lee D. C. (2023). Feasibility design of magnetic auxetic tactile sensor for monitoring the movement of human body, *J. Clinical Research and Clinical Trials*, 8(4).
23. Grima, J.N, and Evans, K.E. (2006). Auxetic behavior from rotating triangles. *Journal of materials science* 41(10):3193-3196.
24. Grima, J.N, and Evans, K.E. (2000). Auxetic behavior from rotating squares. *Journal of materials science letters* 19, 1563-1565.

25. Mizzi L, Spaggiari A and Dragoni E. (2019). Design-oriented modelling of composite actuators with embedded shape memory alloy Compos. Struct. 213:37-46.
26. Mizzi L, Hoseini S. F, Forminghieri M. and Spaggiari A. (2023). Development and prototyping of SMA-metamaterial biaxial composite actuators, Smart Mater. Struct, 32(3):035027.
27. Souza A C, Mamiya E N and Zouain N. (1998). Three-dimensional model for solids undergoing stress-induced phase transformations Eur. J. Mech. A, 17:789-806
28. Auricchio F and Petrini L. (2002). Improvements and algorithmical considerations on a recent three-dimensional model describing stress-induced solid phase transformations Int. J. Numer. Methods Eng, 55:1255-1284.



This work is licensed under Creative Commons Attribution 4.0 License

To Submit Your Article Click Here:

[Submit Manuscript](#)

DOI:10.31579/2693-4779/179

Ready to submit your research? Choose Auctores and benefit from:

- fast, convenient online submission
- rigorous peer review by experienced research in your field
- rapid publication on acceptance
- authors retain copyrights
- unique DOI for all articles
- immediate, unrestricted online access

At Auctores, research is always in progress.

Learn more <https://auctoresonline.org/journals/clinical-research-and-clinical-trials>